IJE TRANSACTIONS C: Aspects Vol. 30, No. 12, (December 2017) 1903-1910

International Journal of Engineering

Journal Homepage: www.ije.ir

High Reynolds Viscous Flow Simulation Past the Elliptical Airfoil by Random Vortex Blob

B. Zafarmand*[a], N. Ghadirzad[b]

[a] Department of Mechanical Engineering, Institute of Energy & Hydro Technology (IEHT), Mashhad, Iran
[b] Department of Mechanical Engineering, Islamic Azad University of Mashhad, Mashhad, Iran

PAPER INFO

Paper history:
Received 18 February 2017
Received in revised form 09 September 2017
Accepted 12 October 2017

Keywords:
Turbulent Viscous Flow
Elliptical Airfoil
Cylinder
Random Vortex Blob

ABSTRACT

In this paper, numerical simulation for a two-dimensional viscous and incompressible flow past the elliptical airfoil is presented by Random Vortex Blob (RVB). RVB is a numerical technique to solve the incompressible, two-dimensional and unsteady Navier-Stocks equations by converting them to rotational non-primitive formulations. In this method, the velocity vector at a certain point can be calculated without considering any grid around it, so the RVB method can be treated as a meshless method. Accordingly, the turbulent flow past a cylinder as well as an elliptical airfoil is investigated. In both cases, the obtained mean time velocities are compared with available numerical and experimental results where an acceptable agreement is observed. Having known the velocity field, by employing momentum balance, the drag and lift coefficients caused by flow past the elliptical airfoil with different diameter ratios and $Re=10^5$ are calculated and compared with experimental data where a good consistency is achieved.

doi: *10.5829/ije.2017.30.12c.12*

1. INTRODUCTION

The elliptical airfoils have developed the rotary wing aircrafts widely which have gained a crucial role in modern military and civil tactics. These airfoils especially have been used for developing and designing the heliplane aircrafts [1].

The study about elliptical airfoils started from 1929, where Zahm et al. [2] studied the elliptical airfoils in wind tunnel and found the drag and lift forces for special conditions. Hantsche and Wendt [3] found the compressible potential flow past the elliptical cylinder at zero angle of attack with no circulation. Johnson et al. [4] used a numerical method for studying the vortices behind the elliptical airfoils for low Reynolds number fluid flow. The turbulent viscous fluid flow past the elliptical airfoils was simulated and Navier-Stocks equations were solved with two dimensional and incompressible fluid assumptions by Kim and Sengupta [5]. Kown and Park [6] found the aerodynamic characteristics of elliptic airfoils at low Reynolds numbers in wind tunnel, but they did not find the velocity field and distribution around the airfoils. Assel [1] calculated the drag and lift forces by using the Fluent software past the elliptical airfoils for various angles of attack. Razaghi et al. [7] investigated the numerical simulation, modeling and optimization of aerodynamic stall control on a NACA0015 airfoil using a synthetic jet actuator. Askari and Shojaeefard [8] presented a mathematical solution for analyzing the potential flow over a rotating cylinder by direct solution of the Laplace's equation. Mehmood et al. [9] studied the NACA0015 airfoil for diffuser design in tidal current turbine application. Chen et al. [10] considered the application of blowing over a thick elliptical airfoil for the purpose of identifying the hierarchy of additional parameters affecting the flow. Lysak et al. [11] measured the unsteady lift spectrum for airfoils in turbulent in a water tunnel experiment. The results provide validation data for analytical models that account for the effect of airfoil thickness on the high frequency gust response. Moreover, in the field of flow

*Corresponding Author's Email: br.zafarmand@gmail.com (B. Zafarmand)

Please cite this article as: B. Zafarmand, N. Ghadirzad, High Reynolds Viscous Flow Simulation Past the Elliptical Airfoil by Random Vortex Blob, International Journal of Engineering (IJE), TRANSACTIONS C: Aspects Vol. 30, No. 12, (December 2017) 1903-1910

past other obstacle, some researches can be found in the literature [9, 12, 13].

One of the most accurate and prosperous methods for simulation of unsteady two-dimensional viscous flow is Random Vortex Blob (RVB). The primary researches can be found in the work of Chorin [14] that analyze the Navier-Stocks equations with RVB. He recommended the method in their famous paper [15]. Bill and Majda [16] studied the convergence of method and increasing the accuracy of simulation that continued with Benfato and Pulvirenti [17]. Chear [18] used this method for fluid flow simulation past an impulsively started cylinder in slightly viscous flow. The published book of Cottet and Koumoutskos [19] expresses the Random Vortex Blob for various geometries and fluid flows. In recent years, some work based on RVB have been performed in other field of engineering [20-23].

The main advantage of Random Vortex Blob is that instant velocity distribution is calculated and then time averaged velocity and velocity fluctuations can be found easily. Calculating velocity fluctuations leads to calculate characteristics of turbulent flow depending on these fluctuations [24]. RVB has advantages and disadvantages. Some of its advantages include: (1) there is no simplification of the equations; (2) contrary to turbulence models, it does not need auxiliary equations; (3) it is used for laminar and turbulent flows; and (4) employing Lagrangian method, it is used to calculate velocity in the high gradient regions. And some of its disadvantages include: (1) because of employing Lagrangian method its computation time is high; and (2) this method cannot be used for three dimensional flows, because it is based on the two dimensional vorticity transport equation which is solved in two steps of convection and diffusion (in the 3D vorticity transport equation the source term exists that cannot be solved in two mentioned steps). Accordingly, in this research, for the first time, RVB is employed in order to calculate the velocity around an elliptical airfoil. Also, a new method is used in order to satisfy the boundary condition on the surface. In this regard, the normal components of velocity are vanished by sources and sinks located on the body of airfoil. After the flow is simulated and vortices move around the airfoil, the velocity field can be found by summation of vortices, sources and sinks induced velocities and potential velocity at each time step. The potential velocity field is an initial condition in this method.

In the current research, the turbulent flow past the elliptical airfoil with various diameter ratios and Reynolds numbers is investigated. Firstly, the instantaneous velocity field is obtained which leads to the calculation of mean time velocity field. Secondly, by the use of instantaneous velocity field and momentum balance, the instantaneous as well as mean drag and lift coefficients are calculated.

2. RANDOM VORTEX BLOB

The RVB is a numerical technique to solve unsteady Navier-Stokes equations converted to a rotational non-primitive formulation and the vorticity transport equation is obtain by operating the curl of Navier-Stokes equations with considering the continuity equation ($\nabla.U = 0$) as:

$$\frac{\partial \omega}{\partial t} + \boldsymbol{U} \cdot \nabla \omega = \frac{1}{\mathrm{Re}} \nabla^2 \omega \tag{1}$$

where ω is dimensionless vorticity, $\boldsymbol{U}$ the vector of velocity, $\mathrm{Re} = U_\infty D/\upsilon$ the Reynolds number, U_∞ the magnitude of the upstream velocity, D the vertical distance cross the flow (the diameter of cylinder or the small diameter of ellipse), υ the kinematic viscosity and t dimensionless time.

It should be stated that the potential velocity is an initial condition and the non-slip condition is used as a boundary condition. The vortices with permanent vorticity vanish the tangential velocity on the surface. After the vortices are created, they move in the flow field and induce the velocity field around themselves and the whole calculating area. Also, the vortices induced the normal component of velocity on the surface at each time step. Thus, in order to eliminate this component the sources and sinks are employed in which they are located in equal distances on the surface. At the first time step, the tangential component of velocity on the segments contains a potential velocity but after the first step due to vortices movement and by using sources and sinks, it also contains vortices, sources and sinks induced velocity.

The vortices move around the body by diffusion and advection mechanisms. This method simulated diffusion by letting the individual vortex blobs undergo independent random walk with the displacement obtained from a Gaussian distribution having zero mean and $\sigma = \sqrt{2t/\mathrm{Re}}$ variance where t is time and Re is the Reynolds number [24], but advection is simulated by calculating the vortices velocity at each time step that contains vortices, sources and sinks induced velocity and potential velocity. For more information about this formulation visit Ref. [24].

3. FORMULATION AND GEOMETRY DESCRIPTION

3. 1. Geometry Figure 1 shows a schematic of parameters investigated in this study. The thickness ratio (t/c) between 0.12 and 0.25 are used for practical usage [6]. Accordingly, the elliptical airfoil section with $t/c = 0.16$ is used in this paper. Also, the inlet flow is considered to be uniform.

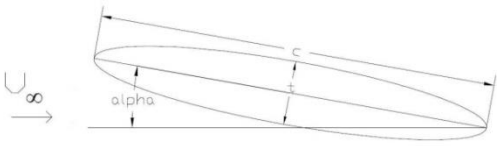

Figure 1. Elliptical airfoil section

3. 2. Vortices Induced Velocity As already mentioned, after the vortices are created, they move around the airfoil, so they induced the velocity field around themselves and the whole calculating area. This induced velocity vectors are obtained as [14, 15]:

$$\bar{W}_{VI}(z_i)=\sum_{j=1}^{N}\frac{-i\Gamma_j|z_i-z_j|}{2\pi\times\max(|z_i-z_j|,\delta)}(\frac{1}{z_i-z_j}) \quad (2)$$

$$i=\sqrt{-1}$$

where δ is the radius of vortices and $\bar{W}_{VI}(z_i)$ an induced velocity vector that N vortices with circulation of Γ_j are making on i^{th} vortex.

3. 3. Sources and Sinks Induced Velocity The vortices induced velocity on the surface at each segment has a normal vector that is eliminated by creating the sources or sinks with specific strength at each segment. Furthermore, this specific strength is obtained with calculating a matrix equations of $A\alpha=b$. The environment of body is divided to M equal segment lengths. So, solving the unknown M equations system lead to producing the M sources or sinks with specific strength on each segment. It should be mentioned that α is the sources or sinks strength matrix, b the vortices induced velocity matrix in each segments with negative sign and A a matrix that comes from the body geometry. The induced velocity with M sources or sinks on the segments at each point of domain can be calculated by [14]:

$$\bar{W}_{SI}(z_i)=\sum_{j=1}^{M}\bar{W}_{SI}(j)$$

$$\bar{W}_{SI}(j)=\begin{cases}\frac{1}{2\pi}\alpha(Q_j)\frac{r(Q_j)}{r^2(Q_j)} & r(Q_j)\geq\frac{1}{2h}\\ \frac{1}{2}h^{-1}\alpha(Q_j)n(Q_j) & r(Q_j)<\frac{1}{2h}\end{cases} \quad (3)$$

where z_i is a point on calculating domain, $\bar{W}_{SI}(j)$ the source and sink induced velocity and $r(Q_j)$ the distance vector from z_i element to the position of certain source or sink.

3. 4. Potential Flow In this study, potential flow around the body is obtained by conformal mapping in complex coordinates. The complex potential function for a circle with radius R by using the conformal function is:

$$F(z)=U_\infty(z+R^2/z) \quad (4)$$

where U_∞ is a velocity of flow far from a body and the complex potential velocity around this circle can be found as:

$$\bar{W}_p(z)=\frac{dF}{dz}=U_\infty(1-\frac{R^2}{z^2}) \quad (5)$$

The function $F(\zeta)$ for the elliptical airfoils is:

$$F(\zeta)=U_\infty(\zeta+\frac{d^2}{\zeta}) \quad (6)$$

where: $d^2=(\frac{a+b}{2})^2$, $a=c$, $b=t$ and for $\zeta(z)$:

$$\zeta(z)=\frac{1}{2}(z+\sqrt{z^2-c^2})e^{i\beta} \quad (7)$$

β is an angle of attack and $c^2=a^2-b^2$. The complex potential velocity around the elliptical airfoils can be given by:

$$\bar{W}_p(z)=u-iv=\frac{dF}{dz}=\frac{U_\infty}{2}(1-\frac{d^2}{\zeta^2})(1+\frac{z}{\sqrt{z^2-c^2}})e^{i\beta} \quad (8)$$

3. 5. Vortices Movement At first, the vortices on the surface move vertically by the diffusion mechanism that works by adding a random number to the new vortices location on the surface. At the next stage, the extant vortices that are separated from the surface, move by both advection and diffusion mechanisms. So, their next location should be found at each time step. The advection mechanism is used by calculating the vortex velocity at each time step which is calculated by summation of vortices, sources and sinks induced velocity and potential velocity at each vortex. If $Z_j(t)$ is a location of vortex in the complex system at t, the vortex location after Δt is [14]:

$$Z_j(t+\Delta t)=Z_j(t)+\left[\bar{W}_p(z_j(t))+\bar{W}_{VI}(z_j(t))+\bar{W}_{SI}(z_j(t))\right]\Delta t+\eta_j \quad (9)$$

where $\bar{W}_{VI}(z_j(t))$ is an induced velocity of other vortices on j^{th} vortex, $\bar{W}_{SI}(z_j(t))$ is an induced velocity of all sources and sinks on j^{th} vortex, $\bar{W}_p(z_j(t))$ is a potential velocity on j^{th} vortex location at t and η_j is a random complex number that is simulating the diffusion mechanism.

3. 6. Lift and Drag Coefficients Aerodynamic drag is exerted on an object when fluid flow passes

through it. This force is due to a combination of the shear and pressure forces acting on the surface of the object. The determination of these forces is difficult since it involves the measurement of both velocity and pressure fields near the surface of the object. However, based on the momentum balance concept, this force can also be determined as carrying out the momentum balance around the object. In order to calculate drag and lift forces, the velocity and pressure on the control surface should be obtained. The surface control is shown in Figure 2. For calculating the mentioned velocities, obtaining the velocity field in the whole domain is not necessary, which is an advantage of RVB method. But, for calculation of pressure and shear stress at each point of surface control, the velocity of four points in the vicinity is needed. The pressure (normalized by ρU_∞^2) on surface number 1 and 3 is given as (the second component of Navier-Stokes equations):

$$\frac{\partial P^*}{\partial y^*}=\frac{1}{\mathrm{Re}}\nabla^2 V^*-\frac{DV^*}{Dt} \tag{10}$$

and for surface number 2 and 4 as:

$$\frac{\partial P^*}{\partial x^*}=\frac{1}{\mathrm{Re}}\nabla^2 U^*-\frac{DU^*}{Dt} \tag{11}$$

It should be stated that the pressure boundary condition at the intersection surface number 1 and 4 is assumed to be zero.

Also, the shear stress on surface number 2 and 4 is obtained as:

$$\tau^*=\frac{1}{\mathrm{Re}}\int\left(\frac{\partial U^*}{\partial y^*}+\frac{\partial V^*}{\partial x^*}\right)dx^* \tag{12}$$

By employing momentum balance and neglecting normal shear stress on the control surface ($\sigma_{xx}^*=(2/\mathrm{Re})\left(\partial U^*/\partial x^*\right)$), the drag coefficient is formulated as:

$$\frac{C_D}{2}=\int_{A_1}\left(P^*+U^{*2}\right)dy^*-\int_{A_3}\left(P^*+U^{*2}\right)dy^*+\int_{A_4}\left(U^*V^*-\tau^*\right)dx^*-\int_{A_2}\left(U^*V^*-\tau^*\right)dx^* \tag{13}$$

Similarly, the lift coefficient is given as:

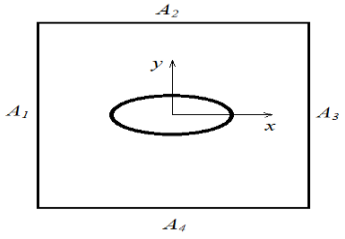

Figure 2. Surface control

$$\frac{C_L}{2}=\int_{A_4}\left(P^*+V^{*2}\right)dx^*-\int_{A_2}\left(P^*+V^{*2}\right)dx^*+\int_{A_1}\left(U^*V^*-\tau^*\right)dy^*-\int_{A_3}\left(U^*V^*-\tau^*\right)dy^* \tag{14}$$

4. RESULTS AND DISCUSSIONS

In this study, the Fortran language is employed for analyzing the turbulent viscous flow past the cylinder and elliptical airfoil section $(t/c=0.16)$ by using the Random Vortex Blob and find the vorticity distribution and vortices moving in different time steps.

The first conclusion of this research indicates the von-Karman street past the cylinder and ellipse truly at an arbitrary time. The vorticity distribution at different time steps for cylinder and ellipse are demonstrated in Figures 3 and 4, respectively. It is assumed that $\Delta t=0.1$ and $\mathrm{Re}=140000$.

According to these figures, it can be observed that the vortices are produced symmetrically behind the body and continued until the beautiful circulation of them is started and the von-Karman street is made. The reason of the curvature changing is the circulation's sign of any vortex that is determined with the sign of instantaneous tangent velocity vector.

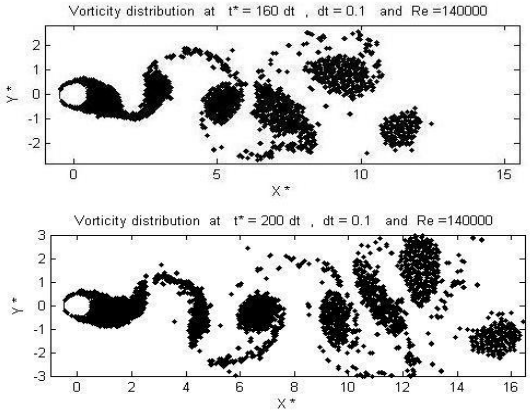

Figure 3. Vorticity distribution at $160\Delta t$ and $200\Delta t$ past the cylindrical airfoil section

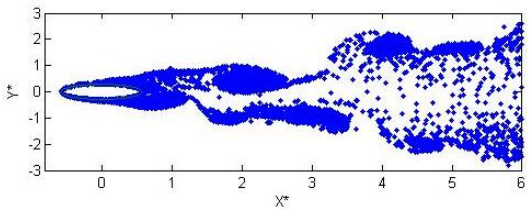

Figure 4. The instantaneous vorticity distribution past the elliptical airfoil section (Re=140000, t/c=0.16)

Also, these Figures show the concentration area reduce by line stream of the body that is the reason of the elliptical airfoil generation to decrease the drag force and the vortex elimination behind the body. The separation zone occupies a small area around elliptical airfoil while the wake zone can be seen in a larger area past the cylinder.

One of the advantages of RVB is visualizing the instantaneous vorticity distribution as well as velocity distribution. In this regard, based on the vorticity distribution, the velocity can be obtained at a certain point or in a fixed network around the body. This velocity distribution shows the accuracy of the code that is implemented by Random Vortex Blob and Fortran language. This mean velocity is compared with the experimental results at $\mathrm{Re}=140000$ for various sections around the cylinder [25], which illustrates the accuracy of the presented simulating method. It is necessary to know that in this code the turbulent flow past the different ellipse can be found by changing the big and small diameters, a (=c) and b (=t). So, by using a=b the turbulent flow past the cylinder can be found.

In Figure 5, the results of mean horizontal velocity and the experimental results for the sections $X^*=0, 0.3, 0.5, 0.6, 1$ are compared with each other. The mean velocity distribution at all points of the network is calculated by summation of potential velocity (W_P), vortex induced velocity (W_{VI}) and sources and sinks induced velocity (W_{SI}) at each point.

Also, the results of mean vertical velocity distributions are shown in Figure 6 for different sections. A good correspondence of experimental and simulating results can be observed. Since there are no experimental results for the turbulent fluid flow past the elliptical airfoil section, the results are compared with the Fluent software results. This problem is simulated by $k-\varepsilon$ method for $\mathrm{Re}=140000$ and maximum iteration of 10 in 50 time steps by Fluent software without any angle of attack.

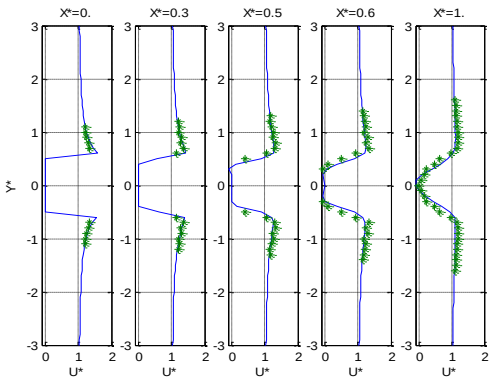

Figure 5. Mean horizontal velocity distributions for different sections around the cylinder (* Experimental result by [27], line is the simulation result by RVB), Re=140000

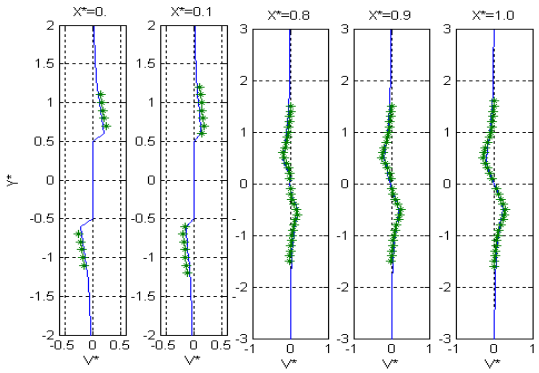

Figure 6. Mean vertical velocity distributions for different sections around the cylinder (* Experimental result by [25], line is the simulation result by RVB), Re=140000

Figures 7 and 8 demonstrate the results for $\mathrm{Re}=140000$, $\Delta t=0.1$ and $t/c=0.16$. In Figure 7, the horizontal average velocities of fluid are plotted. The velocities in the highest and lowest point from the center line ($y^*=0$) in any section are equal to U_∞.

By increasing the distance from the center line, the difference of the horizontal velocity with U_∞ is decreased. Also, this difference is reduced with growing of x^*. In other words, the curvature of average velocity is decreased due to the diminution of boundary layer thickness. Moreover, based on Figure 8, vertical average velocities are symmetric with respect to the center line.

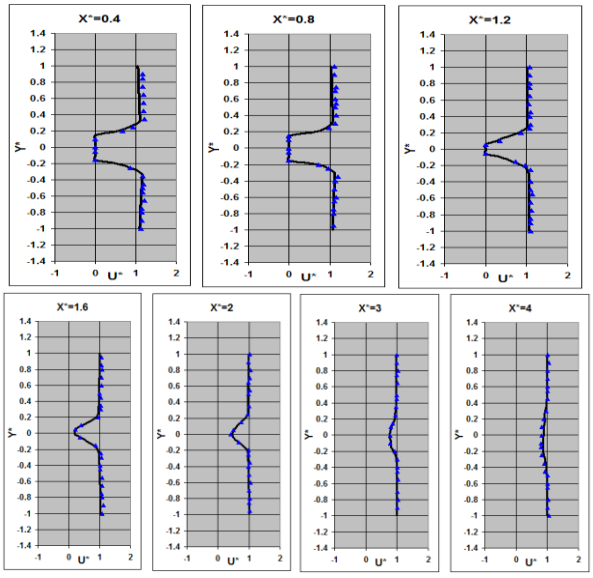

Figure 7. Mean horizontal velocity distributions for different sections around the elliptical airfoil ((▲) Fluent software result, line is the simulation result by RVB) (Re=140000, t/c=0.16)

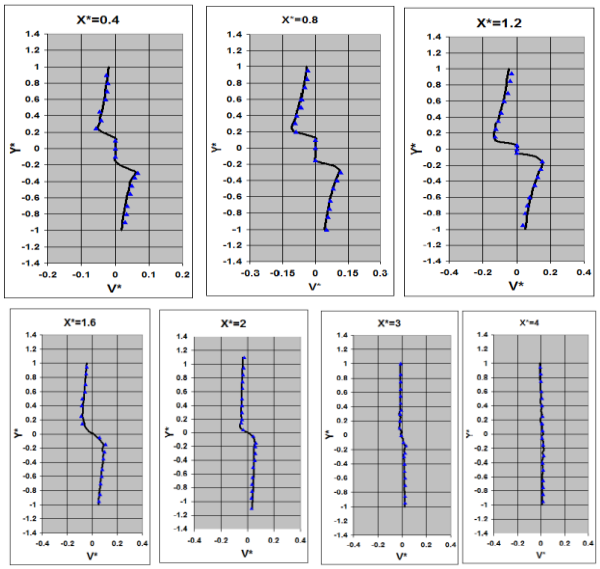

Figure 8. Mean vertical velocity distributions for different sections around the elliptical airfoil ((▲) Fluent software result, line is the simulation result by RVB) (Re=140000, t/c=0.16)

The good results of velocity field achieved from comparing with experimental data indicate that the computational program is evaluating the viscous fluid flow correctly and accurately.

Since the RVB analyses unsteady flow, one of the important applicable results are streamlines and velocity vectors. The instantaneous streamlines is shown at $\mathrm{Re}=140000$ in Figure 9 for cylinder at time= $350\Delta t$ with $\Delta t=0.1$.

By drawing the average streamlines, it can be seen that the irregularity of lines is eliminated and these lines are regular, that is shown in Figure 10 for cylinder. Also, Figure 11 shows the instantaneous velocity vectors for elliptical airfoil section (t/c=0.16) at Re=140000 and time=120Δt and Figure 12 demonstrates average velocity vectors around elliptical airfoil at Re=140000.

Furthermore, Figure 13 illustrates the average velocity vectors for an elliptical airfoil with several angles of attack for $\mathrm{Re}=100000$. According to this figure, by increasing the angle of attack, the wake zone in the bottom half of the geometry becomes smaller while in the upper half gets larger which cause an increase in the lift force.

In order to obtain the drag and lift coefficients (Equations (13) and (14)) of elliptical airfoil, the pressure and shear stress on the surface control is calculated by the use of velocity at each point of it. Since the mentioned velocities are instantaneous, the pressure, shear stress, drag and lift coefficients are obviously instantaneous. So, for calculating mean drag and lift coefficients, 300 successive time steps are averaged.

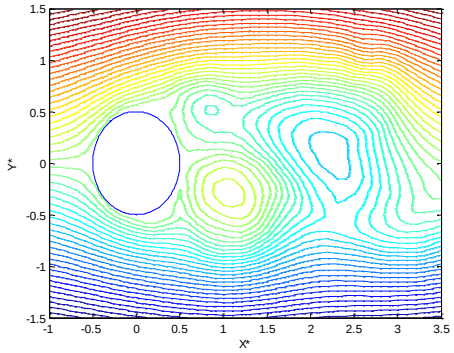

Figure 9. The instantaneous streamlines for cylinder at Re=140000 and time=350Δt

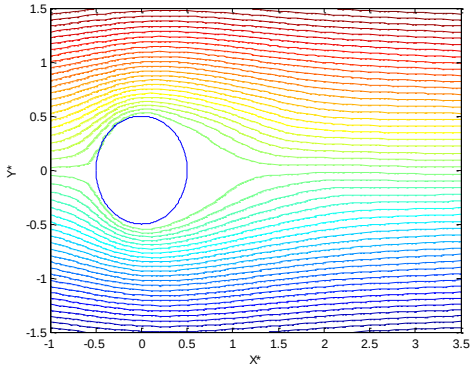

Figure 10. Average streamlines around cylinder at Re=140000

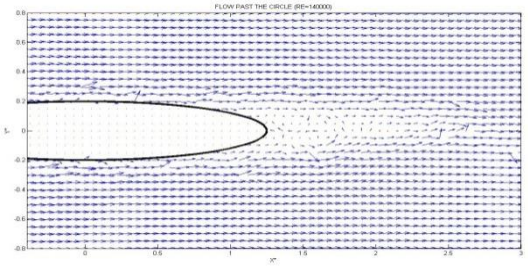

Figure 11. The instantaneous velocity vectors for elliptical airfoil section (t/c=0.16) at Re=140000 and time=120Δt

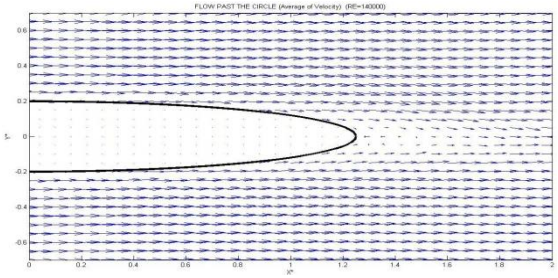

Figure 12. Average velocity vectors around elliptical airfoil at Re=140000

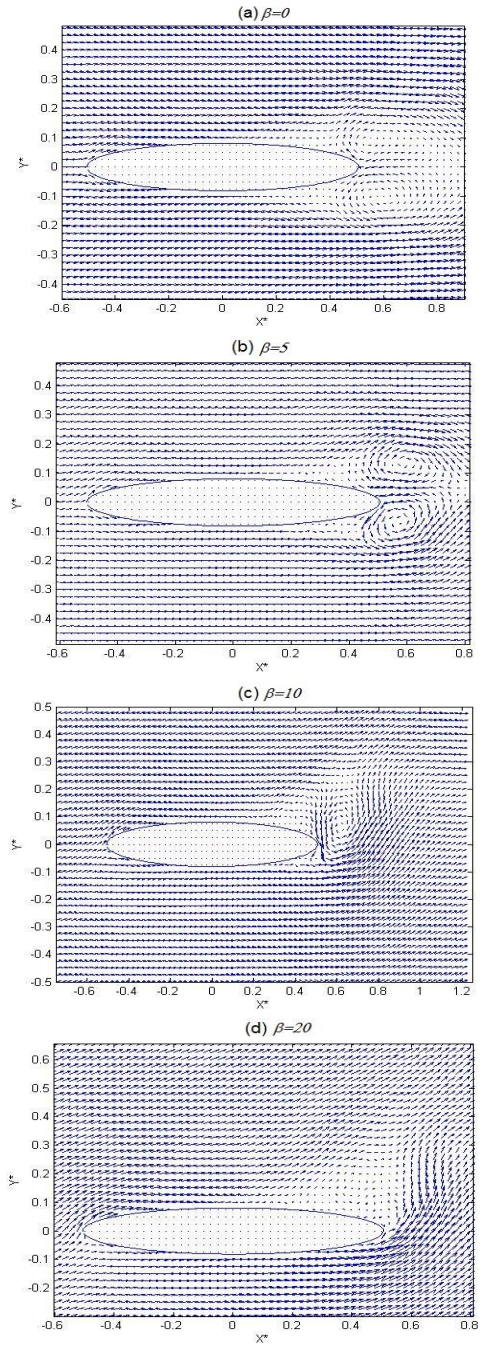

Figure 13. Average velocity vectors around elliptical airfoil with different angles of attack at Re=10^5 (t/c=0.16)

Figure 14 shows mean drag coefficient at Re=10^5 versus different diameter ratios which is compared with experimental data [26]. According to this figure, in constant Reynolds number, with increase of diameter ratio, the drag coefficient is decreased. It should be noted that due to symmetry of geometry (without any angle of attack), the lift coefficient is zero.

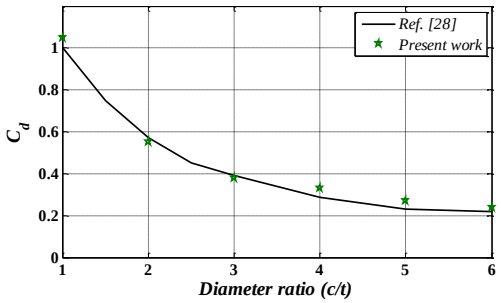

Figure 14. Mean drag coefficient at Re=10^5 versus different diameter ratios compared with Ref. [26]

5. CONCLUSION

In this paper turbulent fluid flow around elliptical airfoil with different angles of attack and cylinder was evaluated and the ability of Random Vortex Blob was indicated. A new method was used in order to satisfy the boundary condition on the surface. In this regard, sources and sinks were considered to vanish the normal component of velocity. Vortex production and vorticity distribution were presented which prove the high ability of RVB for simulation of two-dimensional viscous fluid flow around solid bodies.

Presentation of the average velocity diagrams and the comparison with experimental data and Fluent software results indicate the correct simulation of viscous fluid flow around cylinder and elliptical airfoils. Also, the pressure and shear stress on the surface control was calculated which leads to determine the mean drag and lift coefficients. The mean drag coefficient was compared with experimental results where an acceptable agreement was observed.

6. REFERENCES

1. Assel, T.W., "Computational study of flow over elliptic airfoils for rotor/wing unmanned aerial vehicle applications", Master of Science thesis. Missouri University of Science and Technology, (2007).
2. Zahm, A., Smith, R. and Louden, F., "Forces on elliptic cylinders in uniform air stream", NACA report No. 289, NACA TR-315, (1929).
3. W., H. and H., W., "The compressible potential flow past elliptic cylinder at zero angle of attack and with no circulation", ***Luftfahrtforschung***, Vol. 18, (1942), 311-316.
4. Johnson S.A., M.C., T. and K., H., "Flow past the elliptical cylinder at low reynolds number", in 14th Australasian Fluid Mechanics Conference, Australia. (2001 of Conference).
5. Kim, M.-S. and Sengupta, A., "Unsteady viscous flow over elliptic cylinders at various thickness with different reynolds numbers", ***Journal of Mechanical Science and Technology***, Vol. 19, No. 3, (2005), 877-886.
6. Kwon, K. and Park, S.O., "Aerodynamic characteristics of an elliptic airfoil at low reynolds number", ***Journal of Aircraft***, Vol. 42, No. 6, (2005), 1642-1644.

7. Razaghi, R., Amanifard, N. and Nariman-Zadeh, N., "Modeling and multi-objective optimization of stall control on naca 0015 airfoil with a synthetic jet using gmdh type neural networks and genetic algorithms", ***International Journal of Engineering Transactions A: Basics***, Vol. 22, No. 1, (2009), 69-88.
8. Askari, S. and Shojaeefard, M., "Mathematical modeling of potential flow over a rotating cylinder", ***International Journal of Engineering Transactions A: Basics***, Vol. 24, (2011), 55-63.
9. Mehmooda, N., Lianga, Z. and Khanb, J., "Study of naca 0015 for diffuser design in tidal current turbine applications", ***International Journal of Engineering Transactions C: Aspects***, Vol. 25, No. 4, (2012), 373-380.
10. Chen, C., Seele, R. and Wygnanski, I., "Separation and circulation control on an elliptical airfoil by steady blowing", ***AIAA Journal***, Vol. 50, No. 10, (2012), 2235-2247.
11. Lysak, P.D., Capone, D.E. and Jonson, M.L., "Measurement of the unsteady lift of thick airfoils in incompressible turbulent flow", ***Journal of Fluids and Structures***, Vol. 66, (2016), 315-330.
12. Mirzaee, B., Khoshravan, E. and Razavi, S., "Finite-volume solution of a cylinder in cross flow with heat transfer", ***Algorithms***, Vol. 3, (2002), 303-314.
13. Sabetghadam, F., Soltani, E. and Ghassemi, H., "A fast immersed boundary fourier pseudo-spectral method for simulation of the incompressible flows", ***International Journal of Engineering-Transactions C: Aspects***, Vol. 27, No. 9, (2014), 1457-1466.
14. Chorin, A.J., "Numerical study of slightly viscous flow", ***Journal of Fluid Mechanics***, Vol. 57, No. 4, (1973), 785-796.
15. Chorin, A.J., "Vortex sheet approximation of boundary layers", ***Journal of Computational Physics***, Vol. 27, No. 3, (1978), 428-442.
16. Beale, J.T. and Majda, A., "Rates of convergence for viscous splitting of the navier-stokes equations", ***Mathematics of Computation***, Vol. 37, No. 156, (1981), 243-259.
17. Benfatto, G. and Pulvirenti, M., "Generation of vorticity near the boundary in planar navier-stokes flows", ***Communications in Mathematical Physics***, Vol. 96, No. 1, (1984), 59-95.
18. Cheer, A., "Unsteady separated wake behind an impulsively started cylinder in slightly viscous fluid", ***Journal of Fluid Mechanics***, Vol. 201, (1989), 485-505.
19. Cottet, G.-H. and Koumoutsakos, P.D., "Vortex methods: Theory and practice, Cambridge university press, (2000).
20. Yokota, R. and Obi, S., "Vortex methods for the simulation of turbulent flows", ***Journal of Fluid Science and Technology***, Vol. 6, No. 1, (2011), 14-29.
21. Sohn, S.-I., "Two vortex-blob regularization models for vortex sheet motion", ***Physics of Fluids***, Vol. 26, No. 4, (2014), 044105- 1-20.
22. Ramesh, K., Gopalarathnam, A., Granlund, K., Ol, M.V. and Edwards, J.R., "Discrete-vortex method with novel shedding criterion for unsteady aerofoil flows with intermittent leading-edge vortex shedding", ***Journal of Fluid Mechanics***, Vol. 751, (2014), 500-538.
23. Duan, Y. and Liu, J.-G., "Convergence analysis of the vortex blob method for the b-equation", ***Discrete Contin. Dyn. Syst***, Vol. 34, (2014), 1995-2011.
24. B., Z., M., S. and A., H.N., "Analysis of the characteristics, physical concepts and entropy generation in a turbulent channel flow using vortex blob method", ***International Journal of Engineering Transactions A: Basics***, Vol. 29, No. 7, (2016), 985-994.
25. Cantwell, B. and Coles, D., "A flying hot wire study of the turbulent near wake of a circular cylinder at re= 140000", Ph. D. Thesis, California lnstitute of Technology, (1976),
26. Blevins, R.D., "Applied fluid dynamics handbook", New York, Van Nostrand Reinhold Co., (1984).

High Reynolds Viscous Flow Simulation Past the Elliptical Airfoil by Random Vortex Blob

B. Zafarmand[a], N. Ghadirzad[b]

[a] Department of Mechanical Engineering, Institute of Energy & Hydro Technology (IEHT), Mashhad, Iran
[b] Department of Mechanical Engineering, Islamic Azad University of Mashhad, Mashhad, Iran

P A P E R I N F O

Paper history:
Received 18 February 2017
Received in revised form 09 September 2017
Accepted 12 October 2017

Keywords:
Turbulent Viscous Flow
Elliptical Airfoil
Cylinder
Random Vortex Blob

چکیده

در این مقاله شبیه‌سازی جریان درهم دوبعدی و غیرقابل‌تراکم عبوری از یک بیضی با روش گردابه‌های تصادفی و با استفاده از الگوهای جریان پتانسیل، چشمه، چاه و گردابه بررسی می‌شود. این روش مبتنی بر حل معادله ورتیسیتی دوبعدی و وابسته به زمان می‌باشد و با استفاده از آن می‌توان سرعت را در یک نقطه مشخص بدون کمک و در نظر گرفتن یک شبکه‌بندی بزرگ به دست آورد. لذا می‌توان این روش را یک روش حل معادلات حرکت سیالات بدون شبکه‌بندی برشمرد. ابتدا جریان سیال درهم از روی یک استوانه بررسی، و سپس به جریان درهم عبوری از ایرفویل بیضوی پرداخته می‌شود. در هر دو حالت سرعت‌های متوسط زمانی به دست آمده از مدل با نتایج تجربی و عددی موجود مقایسه شده که تطابق خوبی مشاهده می‌شود. با داشتن میدان سرعت و با استفاده از روش حجم کنترل بالانس مومنتوم، ضرایب درگ و لیفت اعمال شده از سیال بر یک بیضی با نسبت‌های اقطار متفاوت و عدد رینولدز 10^5 محاسبه و با نتایج تجربی مقایسه می‌شود که حاکی از تطابقی رضایت‌بخش است.

***doi**: 10.5829/ije.2017.30.12c.12*